LETTERS

Real-space observation of a two-dimensional skyrmion crystal

X. Z. Yu[1,2], Y. Onose[2,3], N. Kanazawa[3], J. H. Park[4], J. H. Han[4], Y. Matsui[1], N. Nagaosa[3,5] & Y. Tokura[2,3,5]

Crystal order is not restricted to the periodic atomic array, but can also be found in electronic systems such as the Wigner crystal[1] or in the form of orbital order[2], stripe order[3] and magnetic order. In the case of magnetic order, spins align parallel to each other in ferromagnets and antiparallel in antiferromagnets. In other, less conventional, cases, spins can sometimes form highly nontrivial structures called spin textures[4–23]. Among them is the unusual, topologically stable skyrmion spin texture, in which the spins point in all the directions wrapping a sphere[4–7]. The skyrmion configuration in a magnetic solid is anticipated to produce unconventional spin–electronic phenomena such as the topological Hall effect[24–26]. The crystallization of skyrmions as driven by thermal fluctuations has recently been confirmed in a narrow region of the temperature/magnetic field (*T*–*B*) phase diagram in neutron scattering studies of the three-dimensional helical magnets MnSi (ref. 17) and $Fe_{1-x}Co_xSi$ (ref. 22). Here we report real-space imaging of a two-dimensional skyrmion lattice in a thin film of $Fe_{0.5}Co_{0.5}Si$ using Lorentz transmission electron microscopy. With a magnetic field of 50–70 mT applied normal to the film, we observe skyrmions in the form of a hexagonal arrangement of swirling spin textures, with a lattice spacing of 90 nm. The related *T*–*B* phase diagram is found to be in good agreement with Monte Carlo simulations. In this two-dimensional case, the skyrmion crystal seems very stable and appears over a wide range of the phase diagram, including near zero temperature. Such a controlled nanometre-scale spin topology in a thin film may be useful in observing unconventional magneto-transport effects.

The complex spin configurations are of great recent interest[4–23] and are relevant to nontrivial physical phenomena such as the topological Hall effect[24–26]. Their observation and manipulation is therefore an important issue. Spin-polarized neutron scattering has been the most powerful tool to determine spin configurations from information in reciprocal (momentum) space. Ferromagnets and antiferromagnets can easily be analysed in this way, but recent focus is on more complex and non-trivial spin structures for which the analysis is not as straightforward[4–23]. The skyrmion was originally introduced as a model in nuclear physics to describe a localized, particle-like, configuration in field theory[4,5], but it is now highly relevant to the spin structure in condensed-matter systems as well. Its schematic configuration is as shown in Fig. 1c, which pictorially demonstrates that deformation of the two-dimensional (2D) real-space sheet into a unit sphere leads to the spin-direction distribution that wraps around another unit sphere. The number of such wrappings is a topological index, and the skyrmion is therefore topologically stable. The skyrmion spin-system configuration was predicted theoretically[7] in terms of 'vortices' in a magnetic field in crystals with certain crystallographic symmetries. It later turned out that it can appear in various other situations, such as the quantum Hall ferromagnet[8] (as the doped carrier) and cold atoms[9].

In addition to these systems, skyrmions have recently been studied extensively in helical magnets, where the non-collinear spin configuration is realized in the ground state owing to the antisymmetric Dzyaloshinskii–Moriya interaction described by the Hamiltonian[27]

$$H = \int \mathrm{d}\mathbf{r}\left[\frac{J}{2}(\nabla\mathbf{M})^2 + \alpha\mathbf{M}\bullet(\nabla\times\mathbf{M})\right] \quad (1)$$

Here $\mathbf{M}$ is the spatially dependent magnetization (and $(\nabla\mathbf{M})^2 \equiv (\nabla M_x)^2 + (\nabla M_y)^2 + (\nabla M_z)^2$), α is the Dzyaloshinskii–Moriya interaction constant, J is the ferromagnetic exchange coupling and $\mathbf{r}$ is the three-dimensional position vector. The ground state of this Hamiltonian is a helical state with the single wavevector $\mathbf{q}$, which has the fixed magnitude α/J but no fixed direction. The crystal structure produces the anisotropy, but when α/J is small it is weak and the continuum approximation is justified. The spin plane is perpendicular to $\mathbf{q}$, such that H is minimized. This spin structure is called the proper screw. Among many helical magnets, the B20-type transition-metal silicides and germanides (for example MnSi, (Fe,Co)Si and FeGe) with cubic but non-centrosymmetric crystal structure may be good materials in which to test the simple spin model in equation (1). For example, MnSi is a helical magnet owing to the Dzyaloshinskii–Moriya interaction and has an unusual temperature–pressure phase diagram[10–12,14–17]. Neutron scattering shows that under pressure the direction of $\mathbf{q}$ in MnSi is disordered but its magnitude remains constant at $|\mathbf{q}| = 0.043$ Å, resulting in non-Fermi-liquid-like transport properties[14]. The spontaneous skyrmion ground state was theoretically proposed as a candidate for the partially ordered state[15,16]. Recent neutron scattering experiments on MnSi (ref. 17) and $Fe_{1-x}Co_xSi$ (ref. 22) have identified the mysterious 'A phase' with the skyrmion lattice phase. Theoretical analysis and experimental results concluded that the skyrmion lattice is stabilized by thermal fluctuations in some limited region of the *T*–*B* plane near the critical temperature, whereas the conical state with the wavevector $\mathbf{q}$ parallel to the magnetic field is more stable over most of the phase diagram[17].

In comparison with neutron scattering, which provides information about momentum space, real-space observation of magnetic structure using Lorentz transmission electron microscopy (TEM) has the advantage that the single spin texture, as well as the crystallization/melting processes and dislocations of the skyrmion crystal (SkX), can be observed as the temperature and magnetic field are changed. Observation of the helical spin structure in $Fe_{0.5}Co_{0.5}Si$ using Lorentz TEM, including magnetic-lattice defects such as edge dislocations, was first reported in ref. 18. The limitation of TEM is that only the magnetic structure of the electron-transparent thin-plate sample can be detected. Nevertheless, a sample of conventional film thickness

[1]Advanced Electron Microscopy Group and High Voltage Electron Microscopy Station, National Institute for Materials Science, Tsukuba 305-0044, Japan. [2]Multiferroics Project, Exploratory Research for Advanced Technology, Japan Science and Technology Agency, Tokyo 113-8656, Japan. [3]Department of Applied Physics, University of Tokyo, Tokyo 113-8656, Japan. [4]Department of Physics, Sung Kyun Kwan University, Suwon 440-746, Korea. [5]Cross-Correlated Materials Research Group and Correlated Electron Research Group, RIKEN-ASI, Wako 351-0198, Japan.

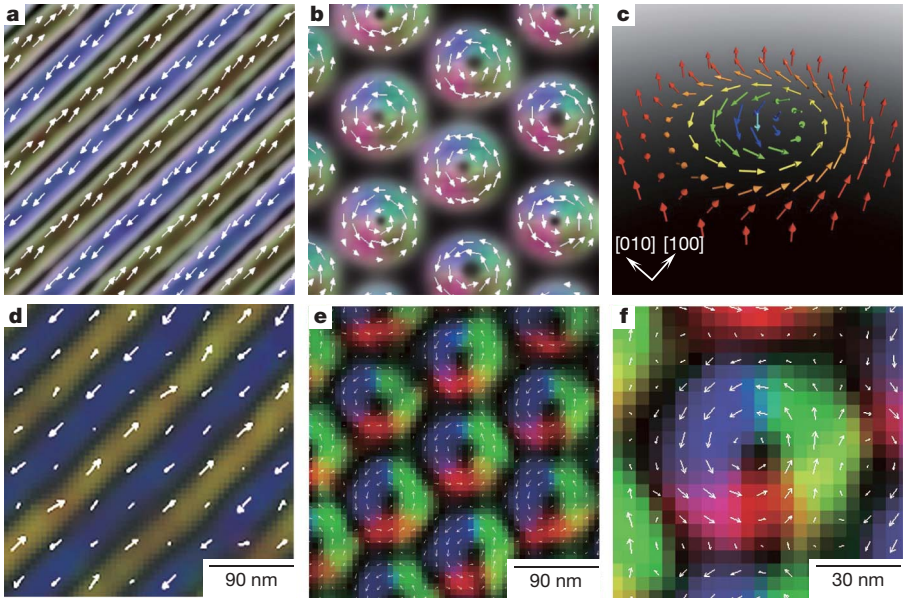

Figure 1 | Topological spin textures in the helical magnet $Fe_{0.5}Co_{0.5}Si$. **a**, **b**, Helical (**a**) and skyrmion (**b**) structures predicted by Monte Carlo simulation. **c**, Schematic of the spin configuration in a skyrmion. **d**–**f**, The experimentally observed real-space images of the spin texture, represented by the lateral magnetization distribution as obtained by TIE analysis of the Lorentz TEM data: helical structure at zero magnetic field (**d**), the skyrmion crystal (SkX) structure for a weak magnetic field (50 mT) applied normal to the thin plate (**e**) and a magnified view of **e** (**f**). The colour map and white arrows represent the magnetization direction at each point.

(several tens of nanometres) can be regarded as a magnetically 2D system, in which the direction of **q** is confined within the plane because the sample thickness is less than the helical wavelength; therefore, various features should appear that are missing in bulk samples. In the context of the skyrmion, the thin film has the advantage that the conical state is not stabilized when the magnetic field is perpendicular to the plane[23]. Therefore, it is expected that the SkX can be stabilized much more easily, and even at $T = 0$, in a thin film of helical magnet.

In this Letter, we report the real-space observation of the formation of the SkX in a thin film of B20-type $Fe_{0.5}Co_{0.5}Si$, the thickness of which is less than the helical wavelength, using Lorentz TEM[28] with a high spatial resolution. The quantitative evaluation of the magnetic components is achieved by combining the Lorentz TEM observation with a magnetic transport-of-intensity equation (TIE) calculation (Supplementary Information).

We first discuss the two prototypical topological spin textures observed for the (001) thin film of $Fe_{0.5}Co_{0.5}Si$. The Monte Carlo simulation (Supplementary Information) for the discretized version of the Hamiltonian in equation (1) predicts that the proper screw (Fig. 1a) changes to the 2D skyrmion lattice (Fig. 1b) when a perpendicular external magnetic field is applied at low temperature and when the thickness of the thin film is reduced to close to or less than the helical wavelength. The Lorentz TEM observation of the zero-field state below the magnetic transition temperature (~40 K) clearly reveals the stripy pattern (Fig. 1d) of the lateral component of the magnetization, with a period of 90 nm, as previously reported[18]; this indicates the proper-screw spin propagating in the [100] or [010] direction. When a magnetic field (50 mT) was applied normal to the plate, a 2D skyrmion lattice like that predicted by the simulation (Fig. 1b) was observed as a real-space image (Fig. 1e) by means of Lorentz TEM. The hexagonal lattice is a periodic array of swirling spin textures (a magnified view is shown in Fig. 1f) and the lattice spacing is of the same order as the stripe period, ~90 nm. Each skyrmion has the Dzyaloshinskii–Moriya interaction energy gain, and the regions between them have the magnetic field energy gain. Therefore, the closest-packed hexagonal lattice of the skyrmion has both energy gains, and forms at a magnetic field strength intermediate between two critical values, each of which is of order α^2/J in units of energy. We note that the anticlockwise rotating spins in each spin structure reflect the sign of the Dzyaloshinskii–Moriya interaction of this helical magnet. Although Lorentz TEM cannot specify the direction of the magnetization normal to the plate, the spins in the background (where the black colouring indicates zero lateral component) should point upwards and the spins in the black cores of the 'particles' should point downwards; this is inferred from comparison with the simulation of the skyrmion and is also in accord with there being a larger upward component along the direction of the magnetic field. The situation is similar to the magnetic flux in a superconductor[29], in which the spins are parallel to the magnetic field in the core of each vortex.

Keeping this transformation between the two distinct spin textures (helical and skyrmion) in mind, let us go into detail about their field and temperature dependences. First, we consider the isothermal variation of the spin texture as the magnetic field applied normal to the (001) film is increased in intensity. The magnetic domain configuration at zero field is shown in Fig. 2a. In analogy to Bragg reflections observed in neutron scattering[22], two peaks were found in the corresponding fast Fourier transform (FFT) pattern (Fig. 2e), confirming that the helical axis is along the [100] direction. In the real-space image, however, knife-edge dislocations (such as that marked by an arrowhead in Fig. 2a) are often seen in the helical spin state, as pointed out in ref. 18. When a weak external magnetic field, of 20 mT, was applied normal to the thin film, the hexagonally arranged skyrmions (marked by a hexagon in Fig. 2b) started to appear as the spin stripes began to fragment. The coexistence of the stripe domain and skyrmions is also seen in the corresponding FFT pattern (Fig. 2f); the two main peaks rotate slightly away from the [100] axis, and two other broad peaks and a weak halo appear. With further increase of the magnetic field to 50 mT (Fig. 2c), stripe domains were completely replaced by hexagonally ordered skyrmions. Such a 2D skyrmion lattice structure develops over the whole region of the (001) sample, except for the areas containing magnetic defects (Supplementary Information). A lattice dislocation was also observed in the SkX, as indicated by a white arrowhead in Fig. 2c. The corresponding FFT (Fig. 2g) shows the six peaks associated with the hexagonal SkX structure. The SkX structure changes to a ferromagnetic structure at a higher magnetic field, for example 80 mT (Fig. 2d, h), rendering no magnetic contrast in the lateral component.

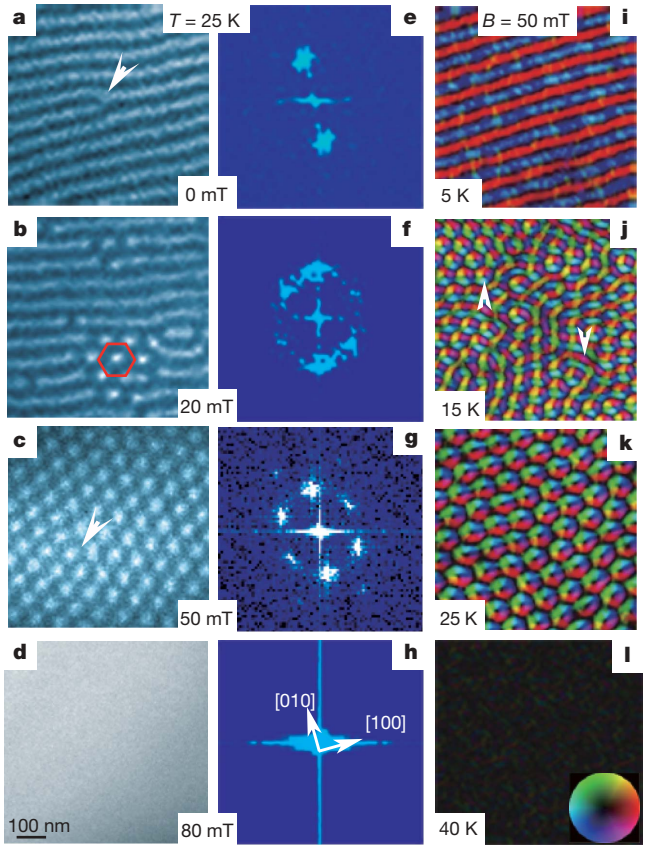

Figure 2 | Variations of spin texture with magnetic field and temperature in $Fe_{0.5}Co_{0.5}Si$. **a–d**, Magnetic-field dependence of the spin texture, in real-space Lorentz TEM (overfocus) images. **e–h**, FFT patterns corresponding to **a–d**. **i–l**, Temperature profiles of the distribution map of the lateral magnetization for a magnetic field of 50 mT. Magnetic fields were applied normal to the (001) thin film. The colour wheel represents the magnetization direction at every point.

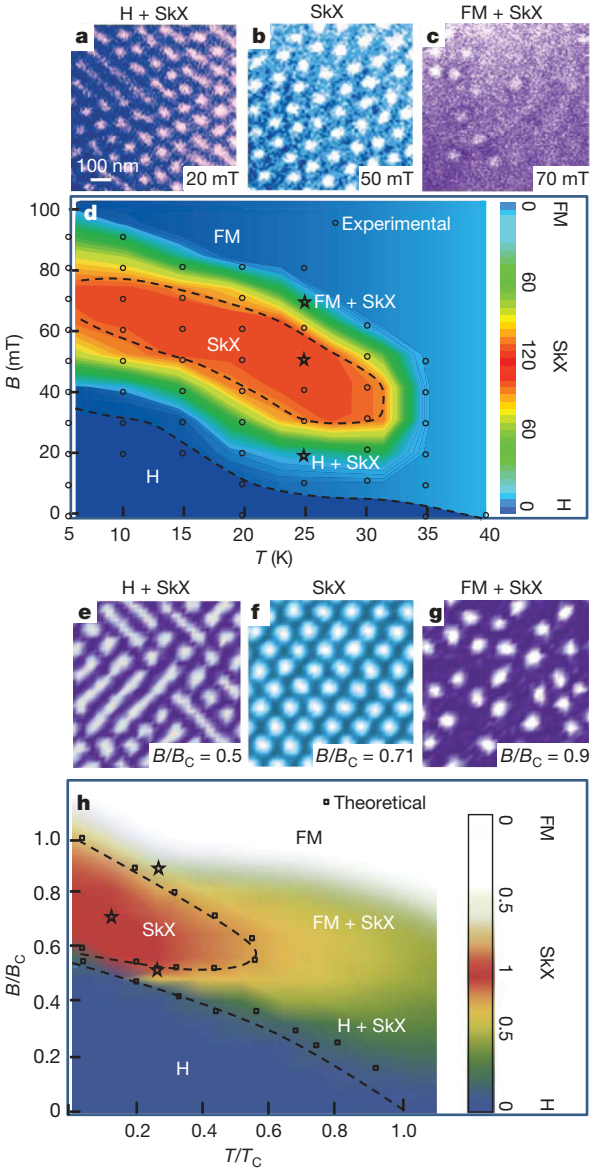

Figure 3 | Phase diagrams of magnetic structure and spin textures in a thin film of $Fe_{0.5}Co_{0.5}Si$. **a–c**, Spin textures observed using Lorentz TEM obtained by Monte Carlo simulation. **e–g**, Spin textures after TEM. H, helical structure; SkX, skyrmion crystal structure; FM, ferromagnetic structure. **d**, **h**, Observed (**d**) and calculated (**h**) phase diagrams in the B–T plane. The magnetic field was applied perpendicular to the image plane. In **h**, B and T are normalized using the arbitrary constants B_C and T_C. The colour bars in the phase diagrams indicate the skyrmion density per 10^{-12} m^2 (**d**) and per d^2 (**h**), d being the helical spin wavelength. Dashed lines show the phase boundaries between the SkX, H and FM phases. Stars in **d** and **h** indicate (T, B) conditions for the images shown in **a–c** and **e–g**, respectively.

Similar skyrmion nucleation and SkX-forming processes were observed as we varied the temperature change at a constant magnetic field (50 mT) applied normal to the film, as shown in the colour-wheel representation (Fig. 2i–l) obtained by our TIE analysis of the Lorentz TEM images. As temperature is increased, the stripy spin texture at 5 K changes to a hexagonal skyrmion crystal at 25 K, through a mixed structure of stripes and skyrmions at 15 K, and the magnetic contrast finally disappears at ~40 K.

The experimental phase diagram for the spin texture for a thin film of $Fe_{0.5}Co_{0.5}Si$, based on the real-space observation, is summarized in Fig. 3d and can be compared with that of the theoretical simulation (Fig. 3h) of the 2D model; in these figures, the phase change of the spin texture is represented as the contour mapping of skyrmion density. The experimental and theoretical results show good agreement not only in the behaviour of the phase change between the helical state and the SkX state (Fig. 3b, f), but also in the transitional coexistence regions of the helical (or ferromagnetic) state and the SkX state; see Fig. 3a, c for the experimental observations and Fig. 3e, g for the theoretical simulation. We see that such a SkX transition, although driven by a weak magnetic field applied perpendicular to the crystal plate plane, also depends on temperature. The SkX phase occupies a larger region of the T–B plane in the experimental phase diagram than in the simulated phase diagram. One possible reason for this is that the pinning effect due to, for example, imperfections in the crystal suppresses the fluctuation of the SkX; this is not taken into account in the simulation. Another possibility, which might be more fundamental, is that the real system has a finite thickness whereas the simulation was carried out for a purely 2D model. The ferromagnetic coupling between the layers effectively increases the spin stiffness in the real case, leading to a 'heavier-spin' object and, consequently, relatively weaker thermal fluctuations than in the 2D model[23].

In a bulk (three-dimensional) crystal, the SkX phase appears in a narrow window of the T–B plane, at around 10 mT and 35–40 K (ref. 19). In comparison with the bulk case, the critical field in the ferromagnetic region is enhanced (up to 100 mT at 5 K) owing to the appreciable demagnetization effect in the 2D case. More significantly, the SkX phase can be produced with a magnetic field normal to the plane even at the lowest temperature. The suppression of the single conical spin state with an applied magnetic field in the 2D system should favour the emergence of the SkX phase, as indicated by the theoretical simulation. We note that the dimension (2D) of the magnetic texture is defined by the thickness of the crystal film being

comparable to (or smaller than) the SkX lattice parameter, which is of the order of 90 nm. Therefore, this situation is most easily realized in the conventional thin-film form of the materials, in which the basic parameters of the spin exchange and the Dzyaloshinskii–Moriya interaction are those of the bulk crystal.

The SkX phase predicted by the theoretical model has been firmly established by direct real-space observation. Spin-structural features including detailed information on nucleation and fusion processes and defects of skyrmions have been revealed. Because such a topological spin texture can be realized in conventional thin-film materials, such materials constitute a new arena in which to test unconventional quantum transport phenomena, such as the enhanced anomalous Hall effect and skyrmion flow, expected for the 2D SkX state.

METHODS SUMMARY

Single-crystal preparation. We grew the $Fe_{0.5}Co_{0.5}Si$ single crystal using the floating-zone technique. The crystal quality was checked by powder X-ray diffraction and energy-dispersive X-ray spectroscopy.

Monte Carlo simulation. Monte Carlo simulation was carried out using a 2D spin model incorporating the Dzyaloshinskii–Moriya interaction and anisotropy (Supplementary Information).

Real-space observation of the skyrmion lattice. We prepared the $Fe_{0.5}Co_{0.5}Si$ thin film using the argon-ion thinning method. The magnetic field applied normal to the thin film was controlled by changing the objective-lens current of the transmission electron microscope. The quantitative evaluation of the magnetic components in the skyrmion lattice was accomplished by combining Lorentz TEM observation with the TIE method (Supplementary Information).

Received 27 January; accepted 23 April 2010.

1. Wigner, E. P. On the interaction of electrons in metals. *Phys. Rev.* **46,** 1002–1011 (1934).
2. Tokura, Y. & Nagaosa, N. Orbital physics in transition-metal oxides. *Science* **288,** 462–468 (2000).
3. Tranquada, J. M. *et al.* Evidence for stripe correlations of spins and holes in copper oxide superconductors. *Nature* **375,** 561–563 (1995).
4. Skyrme, T. A unified field theory of mesons and baryons. *Nucl. Phys.* **31,** 556–569 (1962).
5. Rajaraman, R. *Solitons and Instantons* 115–123 (Elsevier, 1987).
6. Sondhi, S. L., Karlhede, A., Kivleson, S. A. & Rezayi, E. H. Skyrmions and the crossover from the integer to fractional quantum Hall effect at small Zeeman energies. *Phys. Rev. B* **47,** 16419–16426 (1993).
7. Bogdanov, A. N. & Yablonskiĭ, D. A. Thermodynamically stable "vortices" in magnetically ordered crystals. The mixed state of magnets. *Sov. Phys. JETP* **68,** 101–103 (1989).
8. Ho, T. L. Spinor Bose condensates in optical traps. *Phys. Rev. Lett.* **81,** 742–745 (1998).
9. Senthil, T., Vishwanath, A., Balents, L., Sachdev, S. & Fisher, M. P. A. Deconfined quantum critical points. *Science* **303,** 1490–1494 (2004).
10. Ishikawa, Y., Tajima, K., Bloch, D. & Roth, M. Helical spin structure in manganese silicide MnSi. *Solid State Commun.* **19,** 525–528 (1976).
11. Ishikawa, Y. & Arai, M. Magnetic phase diagram of MnSi near critical temperature studied by neutron small angle scattering. *J. Phys. Soc. Jpn* **53,** 2726–2733 (1984).
12. Lebech, B. *et al.* Magnetic phase diagram of MnSi. *J. Magn. Magn. Mater.* **140–144,** 119–120 (1995).
13. Ishimoto, K. *et al.* Small-angle neutron diffraction from the helical magnet $Fe_{0.8}Co_{0.2}Si$. *Physica B* **213–214,** 381–383 (1995).
14. Pfleiderer, C. *et al.* Partial order in the non-Fermi-liquid phase of MnSi. *Nature* **427,** 227–231 (2004).
15. Rößler, U. K., Bogdanov, A. N. & Pfleiderer, C. Spontaneous skyrmion ground states in magnetic metals. *Nature* **442,** 797–801 (2006).
16. Binz, B., Vishwanath, A. & Aji, V. Theory of the helical spin crystal: a candidate for the partially ordered state of MnSi. *Phys. Rev. Lett.* **96,** 207202 (2006).
17. Mühlbauer, S. *et al.* Skyrmion lattice in a chiral magnet. *Science* **323,** 915–919 (2009).
18. Uchida, M., Onose, Y., Matsui, Y. & Tokura, Y. Real-space observation of helical spin order. *Science* **311,** 359–361 (2006).
19. Grigoriev, S. V. *et al.* Magnetic structure of $Fe_{1-x}Co_xSi$ in a magnetic field studied via small-angle polarized neutron diffraction. *Phys. Rev. B* **76,** 224424 (2007).
20. Grigoriev, S. V. *et al.* Crystal handedness and spin helix chirality in $Fe_{1-x}Co_xSi$. *Phys. Rev. Lett.* **102,** 037204 (2009).
21. Takeda, M. *et al.* Nematic-to-smectic transition of magnetic texture in conical state. *J. Phys. Soc. Jpn.* **78,** 093704 (2009).
22. Münzer, W. *et al.* Skyrmion lattice in the doped semiconductor $Fe_{1-x}Co_xSi$. *Phys Rev. B* **81,** 041203(R) (2010).
23. Yi, S. D., Onoda, S., Nagaosa, N. & Han, J. H. Skyrmions and anomalous Hall effect in a Dzyaloshinskii-Moriya spiral magnet. *Phys. Rev. B* **80,** 054416 (2009).
24. Onose, Y., Takeshita, N., Terakura, C., Takagi, H. & Tokura, Y. Doping dependence of transport properties in $Fe_{1-x}Co_xSi$. *Phys. Rev. B* **72,** 224431 (2006).
25. Lee, M., Kang, W., Onose, Y., Tokura, Y. & Ong, N. P. Unusual Hall anomaly in MnSi under pressure. *Phys. Rev. Lett.* **102,** 186601 (2009).
26. Neubauer, A. *et al.* Topological Hall effect in the A phase of MnSi. *Phys. Rev. Lett.* **102,** 186602 (2009).
27. Landau, L. D., Lifshitz, E. M. & Pitaevskii, L. P. *Electrodynamics of Continuous Media* Vol. 8, 178–179 (Elsevier, 2008).
28. Grundy, P. J. & Tebble, R. S. Lorentz electron microscopy. *Adv. Phys.* **17,** 153–242 (1968).
29. Tonomura, A. *et al.* Observation of individual vortices trapped along columnar defects in high-temperature superconductors. *Nature* **412,** 620–622 (2001).

Supplementary Information is linked to the online version of the paper at www.nature.com/nature.

Acknowledgements We would like to thank K. Ishizuka, K. Kimoto, T. Asaka, T. Hara and W. Z. Zhang for discussions. This work was partly supported by the Nanotechnology Network Project (no. ADE21005) and Grants-in-Aid for Scientific Research (numbers 16076205, 17105002, 19019004, 19048008, 19048015, 20046004, 20340086, 21244053 and 22014003) from the Ministry of Education, Culture, Sports, Science and Technology of Japan, and also by the Funding Program for World-Leading Innovative R&D on Science and Technology (FIRST Program). J.H.H. is supported by grants from the Korea Research Foundation (KRF-2008-521-C00085 and KRF-2008-314-C00101).

Author Contributions Y.T. contributed to the planning of the study and the writing of the paper. X.Z.Y. and Y.M. performed the Lorentz TEM observations and wrote the experimental section of the paper. Y.O. and N.K. grew the sample crystal and contributed to the assignment of the Lorentz TEM images. J.H.P., J.H.H. and N.N. did the calculations and wrote a significant part of the discussion.

Author Information Reprints and permissions information is available at www.nature.com/reprints. The authors declare no competing financial interests. Readers are welcome to comment on the online version of this article at www.nature.com/nature. Correspondence and requests for materials should be addressed to X.Z.Y. (yu.xiuzhen@nims.go.jp) or Y.T. (tokura@ap.t.u-tokyo.ac.jp).